NeuroImage 90 (2014) 413–422

Contents lists available at ScienceDirect

NeuroImage

journal homepage: www.elsevier.com/locate/ynimg

fMRI characterization of visual working memory recognition

Benjamin Rahm [a,b], Jochen Kaiser [a], Josef M. Unterrainer [b], Juliane Simon [a], Christoph Bledowski [a,*]

[a] Institute of Medical Psychology, Goethe University, Heinrich-Hoffmann-Strasse 10, D-60528 Frankfurt am Main, Germany
[b] Medical Psychology and Medical Sociology, Johannes Gutenberg University, Duesbergweg 6, D-55128 Mainz, Germany

ARTICLE INFO

Article history:
Accepted 11 December 2013
Available online 19 December 2013

Keywords:
Working memory
Recognition
Attention
Memory
Decision making
fMRI

ABSTRACT

Encoding and maintenance of information in visual working memory have been extensively studied, highlighting the crucial and capacity-limiting role of fronto-parietal regions. In contrast, the neural basis of recognition in visual working memory has remained largely unspecified. Cognitive models suggest that recognition relies on a matching process that compares sensory information with the mental representations held in memory. To characterize the neural basis of recognition we varied both the need for recognition and the degree of similarity between the probe item and the memory contents, while independently manipulating memory load to produce load-related fronto-parietal activations. fMRI revealed a fractionation of working memory functions across four distributed networks. First, fronto-parietal regions were activated independent of the need for recognition. Second, anterior parts of load-related parietal regions contributed to recognition but their activations were independent of the difficulty of matching in terms of sample-probe similarity. These results argue against a key role of the fronto-parietal attention network in recognition. Rather the third group of regions including bilateral temporo-parietal junction, posterior cingulate cortex and superior frontal sulcus reflected demands on matching both in terms of sample-probe-similarity and the number of items to be compared. Also, fourth, bilateral motor regions and right superior parietal cortex showed higher activation when matching provided clear evidence for a decision. Together, the segregation between the well-known fronto-parietal activations attributed to attentional operations in working memory from those regions involved in matching supports the theoretical view of separable attentional and mnemonic contributions to working memory. Yet, the close theoretical and empirical correspondence to perceptual decision making may call for an explicit consideration of decision making mechanisms in conceptions of working memory.

Introduction

The ability to encode and maintain currently relevant information for use in cognition and to guide behavior is termed working memory (Baddeley, 1986; Cowan, 2005). It not only provides a mental workspace for the highest mental functions such as reasoning and planning, but also is used ubiquitously in seemingly effortless everyday actions, for example the detection of a sought-after product in a shop. In order to enable working memory functioning, items must be successfully encoded, maintained and used, e.g. for recognition. Typically, in working memory research delayed-match-to-sample tasks have been applied, comprising three phases reflecting these functions (Sternberg, 1966). During the encoding phase subjects are asked to encode a visual display containing several items, the delay phase requires the maintenance of the previously presented samples, while during the final recognition phase, a test stimulus probes the subjects' memory recognition.

Previous neuroimaging research has primarily focused on the neuronal basis underlying encoding and maintenance functions (Gazzaley and Nobre, 2012). Typically, increased activation was observed in a fronto-parietal network of regions when a higher number of memory items were to be retained (Linden et al., 2003; Todd and Marois, 2004; Xu and Chun, 2006). A pivotal role has been assigned to the posterior parietal cortex along the intraparietal sulcus (IPS) where activation increases with memory load and saturates at the individual memory capacity limit (Todd and Marois, 2004; Xu and Chun, 2006). These activations are not specific to working memory, but widely overlap with the dorsal attention network (Corbetta and Shulman, 2002). Consequently, they are commonly considered as contributing to working memory by providing attentional resources and basic functions such as attentional highlighting and shifting the focus of attention between mental representations (Bledowski et al., 2009; Emrich et al., 2013; Lepsien and Nobre, 2007). Current theoretic models hence propose that working memory emerges from the interaction of attentional and mnemonic processes, with attention supporting (but also limiting) the encoding and the short-term maintenance of mnemonic or sensory representations (Awh et al., 2006; Bledowski et al., 2010; Gazzaley and Nobre, 2012; Ikkai and Curtis, 2011; Linden, 2007; Postle, 2006; Todd and Marois, 2004).

* Corresponding author. Fax: +49 69 6301 7606.
E-mail addresses: rahm@uni-mainz.de (B. Rahm), j.kaiser@med.uni-frankfurt.de (J. Kaiser), unterrai@uni-mainz.de (J.M. Unterrainer), julianesimon1@aol.com (J. Simon), bledowski@em.uni-frankfurt.de (C. Bledowski).

1053-8119/$ – see front matter © 2013 Elsevier Inc. All rights reserved.
http://dx.doi.org/10.1016/j.neuroimage.2013.12.017

In contrast, although essential for our understanding of the neural system mediating working memory, there is a surprising lack of neuroimaging evidence on the recognition of items held in visual working memory (Gazzaley and Nobre, 2012). Especially, it is largely unknown, which role regions supporting maintenance in visual working memory play for recognition.

Based mainly on behavioral observations, working memory recognition has been conceptualized to use the same mechanisms as recognition from episodic memory (McElree, 2006; Oberauer, 2002), thus primarily relying on mnemonic resources. In consequence, the separation of attentional and mnemonic contributions to working memory should hold true in recognition. However, the few existing functional neuroimaging data on visual working memory recognition provide a heterogeneous and incomplete picture. Control experiments conducted in studies on capacity limitations of working memory speak against a strong role of attentional regions (i.e. IPS) for recognition (Todd and Marois, 2004; Xu and Chun, 2006). These studies, however, were based on region-of-interest analyses, and hence did not shed light on the question which regions actually do subserve recognition. In contrast, others have reported memory load-related fronto-parietal activation for the recognition phase (Bledowski et al., 2006; Linden et al., 2003). Yet, to our knowledge, none of these studies has shown that this activation was actually related to recognition, and was not due to other processes that operate in temporal proximity to the time point of recognition, such as anticipatory attentional resource allocation or the reactivation of the memory contents just before the expected probe onset (Kaiser et al., 2009a,b).

Therefore, a first goal of the present study was to clarify the role that fronto-parietal regions typically involved in maintenance play in recognition. To this end, we varied memory load to produce load-related fronto-parietal activations, while independently manipulating the need for recognition and recognition demands: in a delayed-match-to-sample task, participants encoded either one or three colors and after a short delay were confronted with a probe item that either did or did not entail recognition (see Fig. 1a). If the dorsal attention network actively contributes to recognition, it can be expected to show a stronger activation when recognition is required than when it is not. Otherwise, if memory load-related increases in activation are independent of the need for recognition, they might rather reflect the demands of the earlier task phase.

Our second goal was to specify the neural basis of recognition in visual working memory on the whole-brain level. The conceptual core of recognition consists of a mechanism that matches incoming sensory information (the probe stimulus) to internal representations held in visual working memory. Models of this matching mechanism consider it as a process of accumulating evidence for the agreement of the probe to the samples held in memory (Kahana and Sekuler, 2002; Nosofsky, 1988; Ratcliff, 1978). If the degree of accordance exceeds a critical threshold, participants will respond "yes, the probe corresponds to one of the samples". Matching hence critically depends on the similarity between probe and sample(s). We therefore systematically varied sample-probe similarity to characterize the neural correlates of the matching process. Specifically, the probe on each trial was either dissimilar to all memory items, similar to one item or identical with one item held in memory.

Notably, these matching models are not exclusively applied to working memory tasks. Rather, they were designed and used to model the speed and accuracy of perceptual decision making/categorization and long-term memory recognition. Both perceptual decision making and long-term recognition are associated with widely overlapping brain responses encompassing posterior cingulate cortex/precuneus (PCC/PCN), superior frontal sulcus (SFS) and temporo-parietal junction (TPJ) (for reviews, see Heekeren et al., 2008; Wagner et al., 2005). If the results of the present study reproduce a similar pattern, this would provide descriptive support for the assumed generality of these models.

Finally, as both memory load and sample-probe similarity increase the demands on recognition, we examined whether these different sources of increased demands would yield common activations, which would support the notion of a generalized matching mechanism. Alternatively, a larger number of representations to be mentally searched (as imposed by memory load), and a higher necessary precision of the matching process (as imposed by sample-probe-similarity) may recruit different mechanisms.

In summary, this study examined working memory recognition by (1) testing whether the dorsal attention network that is typically observed during encoding and maintenance also contributes to recognition, and by (2) providing a detailed characterization of its neural basis.

Materials and methods

Participants

21 right-handed participants (mean age = 26.8 (SD = 3.65); 12 females) participated in the study. All reported normal or corrected-to-normal visual acuity and the absence of any history of neurological or psychiatric disorders and psychotropic medication. Participants were

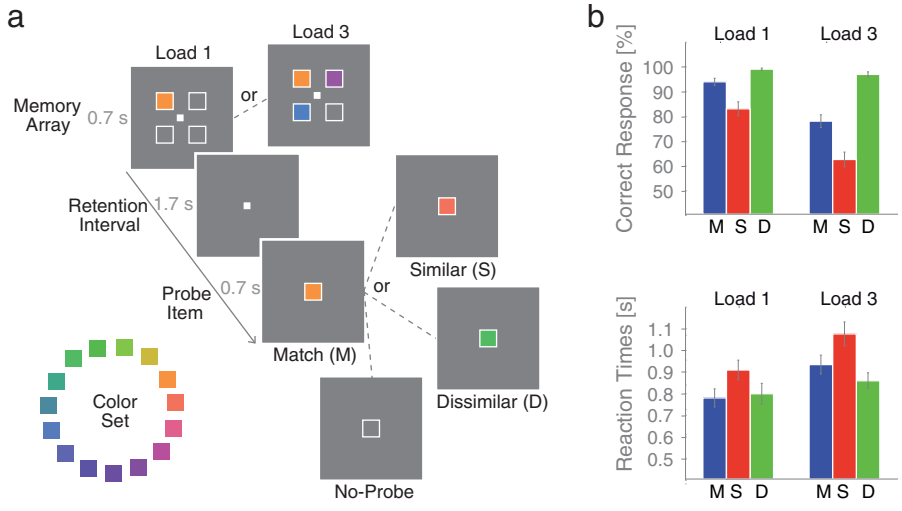

Fig. 1. Experimental design and mean behavioral performance by condition. (a) Subjects encoded and retained either 1 or 3 colors for a short delay of 1.7 s. Independent of memory load, the surface color of the probe square was varied to determine demands on recognition. A gray probe square indicated no need for recognition and response (No Probe). Alternatively (probe trials), the probe's color could match one of the items held in memory (M), be similar, but visually clearly discernible to one of the memoranda and dissimilar to all others (S), or be dissimilar to all memory items (D). Subjects judged whether the probe matched any of the encoded color(s) or not and responded by button press. (b) Percentage of correct responses and RTs are plotted against memory load condition and probe type. Error bars indicate ±1 SEM.

screened for deficits in color vision with the colors used in the main experiment, presented at the same size. None of them showed difficulties in perceptually discriminating these colors. Written informed consent was obtained from each participant. The study was approved by the ethics committee of the University of Frankfurt Medical Faculty.

Study design

The study employed a standard three-phase delayed match-to-sample task, comprising encoding of samples, their short-term maintenance and finally testing of memory by presentation of a probe stimulus that was to be matched against the memoranda (see Fig. 1a). Each trial was composed of 0.7 s of encoding, 1.7 s of maintenance and 0.7 s of probe presentation, followed by a variable intertrial interval of 2.4 to 6 s that was included to separate the hemodynamic responses of adjacent trials.

The study design incorporated independent variations of the number of memory items to encode and retain, and the degree of similarity between the memory items and the probe. At encoding, either one or three colors ("low" vs. "high" load) had to be memorized. Independent of load, four small white squares (about 1.5° × 1.5° of visual angle) were presented parafoveally (eccentricity of about 4.2° × 4.2° of visual angle) on a dark gray background, of which either one or three were filled with different, dissimilar colors. Positions of the to-be-encoded items were pseudo-randomized, ensuring an equal distribution across trials and levels of memory load. During the subsequent delay phase, only the fixation cross remained on the screen. At recognition, a single white-bordered, colored square was presented foveally, that was to be matched against the stored representations of the encoded memory items. Independent of memory load, the surface color of the probe square was chosen to vary the demands on recognition. A gray probe square indicated no need for recognition and response ("no-probe trials" (NP)). Alternatively, the probe's color could match one of the items held in memory ("matching-probe trials" (M)), be similar, but visually clearly discernible to one of the memoranda and dissimilar to all others ("similar-probe trials" (S)), or be dissimilar to all memory items ("dissimilar-probe trial"(D)). The task of the participants was to decide whether the presented probe was identical to one of the colors memorized at encoding and to indicate their decision as quickly as possible without sacrificing accuracy by pressing the "match" or the "non-match" button with the index or middle finger of their right hand, respectively.

The used colors were selected on the basis of pilot testing, by starting from an isoluminant set, that was gradually altered to have a "circle" of at least 15 colors available that were clearly discriminable perceptually (Fig. 1a). Importantly, we ensured that each color was perceptually more similar to its two neighbors on the "circle" than to non-neighboring colors (that is, colors that were separated by one or more intermediate colors). This enabled us to manipulate the similarity between a memory color and a probe stimulus by varying their distance on the color circle. The term "similar" refers to directly neighboring colors, whereas "dissimilar" denotes that colors were separated by at least one intermediate color (please see Supplementary Table 1 for CIE Yxy color coordinates of the used colors, as measured with a Konica Minolta CS100A chromameter).

Memory items were pseudo-randomly drawn from the resulting set of 15 different colors. We ensured that all sample colors were dissimilar to each other, by requiring that each memory item was separated from the others by at least three intermediate colors on the circle. (Note that the "middle" one of these three would still be dissimilar to all memory items). The probe color's distance to the nearest memory item was controlled to be zero (matching trials), one (similar trials) or at least two (dissimilar trials). In consequence, even under high memory load, three colors plus their six neighbors were matching or similar, still leaving six potential dissimilar probe colors, rendering probe prediction impossible. Furthermore, the distance of each probe to all other items was ensured to lie in the range of dissimilar colors. Sample-probe similarity was sufficiently defined for our aims and – as the probe was similar to/matching only one memory item – was equivalent for both memory load levels. In contrast, a purely random selection of colors would have resulted in a vast increase of item-probe similarity with increasing load. This sampling phenomenon is evident in all materials with a limited feature space, such as colors, faces, houses and random shape outlines. Apart from sample-probe similarity, the importance of the similarity between memory items has been emphasized (Kahana and Sekuler, 2002). As described above, all memory items were dissimilar to each other, hereby keeping the inter-item distance high across trials and effectively minimizing its potential influence on high as opposed to low load trials.

Data acquisition

High-resolution (1 mm^3) anatomical and functional scans were taken using a 3 T Siemens (Munich, Germany) Allegra MR scanner with a standard birdcage headcoil. 23slices (3.125 × 3.125 × 5 mm, 0.5 mm slice separation, TR 1,200 ms, TE 26 ms, flip angle 80°) effectively covering the whole cerebrum were attained. The scanning sequence included an online distortion correction (based on a fieldmap acquired before the functional scans) and realignment of scans for subject motion (Zaitsev, Hennig and Speck, 2004).

Four runs comprising 600 scans each were performed. After the second functional scan the anatomical scan was conducted to allow for a short recovery period for the participant. The first 5 scans of each run were discarded to take into account the time until steady-state tissue magnetization was reached.

Stimuli were presented using an MR-compatible goggle system with two organic light-emitting diode displays (MR Vision 2000; Resonance Technology, Northridge, USA). Presentation software (Neurobehavioral Systems, Albany, USA) was used to present stimuli and record manual responses.

Data analysis

Behavioral data

Each participant's percentage of correct responses data for each condition was computed. Response times were aggregated using the mean of correct trials for each condition. Mean-aggregated response times and individual percentage of correct responses were then entered into separate 2 (memory load) × 3 (sample-probe similarity) repeated-measures ANOVAs using SPSS software (IBM Corp., Chicago, USA).

MRI data

MRI data were analyzed using SPM8 (Wellcome Department, http://www.fil.ion.ucl.ac.uk/spm). For preprocessing, data were converted, realigned, and coregistered to the individual anatomical image. The anatomical image was segmented and normalized with the VBM8-toolbox (http://dbm.neuro.uni-jena.de) using the DARTEL approach (diffeomorphic anatomical registration through exponentiated lie algebra; Ashburner, 2007). The resulting transformations were applied to the functional scans which included re-sampling to isotropic 1.5 mm^3 voxels and smoothing with an isotropic Gaussian kernel (full-width at half-maximum, FWHM = 8 mm).

For first level analysis, individual effects were estimated using the general linear model approach implemented in SPM8, including a high-pass filter with a cutoff frequency of 1/128 Hz and correction for non-independence between adjacent scans by use of an AR-model. For each run, the individual models included the following predictors: 6 predictors for correct trials in the single conditions resulting from the combination of memory load (1 vs. 3) and sample-probe similarity (matching, similar, dissimilar probes), 2 predictors for no-probe trials at memory load 1 and memory load 3, 1 predictor containing all erroneous trials and RT outliers and six subject-motion regressors. Note that these motion regressors did not reflect the realignment parameters obtained in SPM for the scans that had already been motion-corrected during

data acquisition, but resulted from realigning the series of motion-uncorrected scans that is additionally output by the scanner.

Instead of assuming a fixed shape of the hemodynamic response, we used scan-wise modeling of the individual effects via a finite impulse response model. For each of the 13 scans following the onset of the encoding phase, a separate regressor was entered into the model, in total modeling 15.6 s after stimulus onset, which covered the bulk of the hemodynamic response.

For second level random-effects group analysis, individual contrasts of the scans 6 to 8 of each condition versus implicit baseline were computed. Scans 6 to 8 span the range from 3.6 to 7.2 s after presentation of the probe, and should comprise the peak of the hemodynamic response even in the presence of some interregional variability. The resulting contrast maps were entered into a repeated-measures ANOVA. The ANOVA consequently included three factors of memory load (2 levels: load 1, load 3), sample-probe similarity (4 levels: match, similar non-match, dissimilar non-match, no-probe) and scan (3 levels: 6 to 8). Multi-line F-contrasts were then used to identify effects that were present at least in one of the scans 6 to 8. For identification of differential load effects that depend on whether or not recognition was required, matches, similar non-matches and dissimilar non-matches together were contrasted to no-probe trials. In order to detect activations that depended on specific demands amongst conditions requiring recognition, variance associated to differences between matches, similar non-matches and dissimilar non-matches was analyzed.

Correction for multiple comparisons was performed using a false-discovery rate of $p < 0.05$. Assignment of MNI coordinates to anatomical brain regions were made with the wfu pick atlas toolbox (http://fmri.wfubmc.edu/software/PickAtlas; Maldjian, Laurienti, Kraft and Burdette, 2003).

Results

Behavioral data

Response times and accuracy were analyzed using 2 (memory load) × 3 (sample-probe similarity) repeated-measures analyses of variance (ANOVA), including Greenhouse–Geisser correction for non-sphericity when indicated. Results are illustrated in Fig. 1b. For memory load we observed main effects with decreased accuracy ($F(1,20) = 195.9$; $p < 0.001$; mean ± s.e.m.: Load 1: 92.1% ± 1.0, Load 3: 79.2% ± 1.2) and increased response times ($F(1,20) = 92.7$; $p < 0.001$; Load 1: 829.9 ms ± 42.9; Load 3: 956.7 ms ± 43.0) when three instead of one item had to be retained.

Likewise the main effect of similarity proved significant for both accuracy ($F(1.2,23.6) = 47.5$; $p < 0.001$) and RT ($F(2,20) = 33.5$; $p < 0.001$). Recognition judgments were most accurate for dissimilar probes (98.1% ± 0.7), followed by matches (86.1% ± 1.6) and least accurate for similar probes (72.9% ± 2.6). Pairwise comparisons showed that all three probe categories differed significantly ($p < 0.05$, Bonferroni-corrected). Response times for matches (857 ms ± 41) and dissimilar probes (829 ms ± 42) did not differ significantly, but both were processed faster than similar probes (993 ms ± 49).

Finally, a significant memory load × sample-probe similarity interaction for both performance measures (accuracy: $F(1.4,28.7) = 15.6$; $p < 0.001$; RT: $F(2,40) = 8.4$; $p < 0.001$) indicated that the memory load effect on recognition was conditional on sample-probe similarity. Specifically, as revealed by post-hoc comparisons ($p < 0.05$, Bonferroni-corrected), recognition accuracy dropped more sharply under high memory load for matches (Load 1: 94.1% ± 1.4; Load 3: 78.1% ± 2.6) and similar probes (Load 1: 83.2% ± 2.8; Load 3: 62.6% ± 3.0) than for dissimilar probes (Load 1: 99.1% ± 0.4; Load 3: 97.0% ± 0.1). Likewise, from low to high memory load, response times for matches (Load 1: 781 ms ± 42; Load 3: 934 ms ± 43) and similar probes (Load 1: 909 ms ± 46; Load 3: 1076 ms ± 55) increased more strongly than for dissimilar probes (Load 1: 800 ms ± 48; Load 3: 860 ± 37).

In summary, as expected, both higher memory load and increased sample-probe similarity led to longer response times and decreased recognition accuracy. Also, memory load and sample-probe similarity were shown to interact. Whereas a pronounced memory load effect was evident for matches and similar probes, the impact of memory load was clearly reduced for dissimilar probes.

fMRI results

Variation of memory load was most often used to examine memory encoding and maintenance. Here we sought to evoke load-dependent activations to evaluate their role for recognition. Moreover, in combination with sample-probe similarity, it may reveal whether different manipulations of recognition difficulty tap into common neural resources and thus serve to characterize the neural basis of recognition from working memory.

Effects of memory load

As expected, comparing high to low memory load reproduced the well-known widespread activation across fronto-parietal regions (Fig. 2a, Table 1 and Supplementary Table 2). Due to the fixed sequence of phases of the delayed-match-to-sample task and the temporally protracted course of the BOLD response, however, these activations cannot unequivocally be attributed to recognition. Rather they may have been carried over from the delay phase or result from preparatory processes just before the expected onset of probe presentation. To resolve this issue, we incorporated no-probe trials into our design: these were identical to all other trials until the end of the delay phase, but then did not demand probe recognition from working memory. They may hence serve as a reasonable measure of whether observed memory load-related activations were actually attributable to recognition. If memory load affected brain activation in both probe and no-probe trials (conjunction analysis, FDR-corrected for multiple comparisons, $p < 0.05$), and moreover, activations did not differ between probe and no-probe trials even at an extremely liberal threshold of $p < 0.1$, uncorrected for multiple comparisons, we would consider the resulting activations as most likely not systematically related to recognition. Putting these considerations to test, activations were found in bilateral posterior parietal cortex along the posterior part of the intraparietal sulcus (posterior IPS) and superior parietal lobule as well as at the intersection of precentral and superior frontal sulci, putative human frontal eye fields (FEF), and right anterior middle frontal gyrus. Fig. 2a depicts these activations in purple. In addition, Fig. 2c (first row, left and middle panel) shows activation time courses in right FEF and right posterior IPS that illustrate similar activity modulations in probe and no-probe trials. The full set of cortical and subcortical coordinates is listed in Table 1 and Supplementary Table 2, first section, respectively. Together, these results argue against a strong involvement of posterior IPS and FEF in recognition, which is in sharp contrast to their pivotal role during memory encoding/maintenance.

But which load-responsive brain regions are involved in recognition? As a minimum requirement a memory load effect should be evident at least in probe trials. Additionally stronger responses should be observed when recognition was demanded (probe trials) than when it was not required (no-probe trials). Computing this conjunction analysis revealed widespread activations in frontal, parietal and temporal cortices. They are shown in green in Fig. 2a. The full set of activation coordinates is listed in Table 1 and Supplementary Table 2, second section, respectively.

To segment this large-scale pattern into potentially meaningful functional components, we explored activations by grouping them into two sets that differed with respect to whether they (1) additionally showed a memory load effect in no-probe trials at $p < 0.001$ (uncorrected), or (2) did not exhibit any sign of a memory load effect ($p > 0.1$, uncorrected). As no-probe trials did not demand recognition, any memory load effect observed in these trials will probably be imported from the encoding or maintenance phases of the task. In

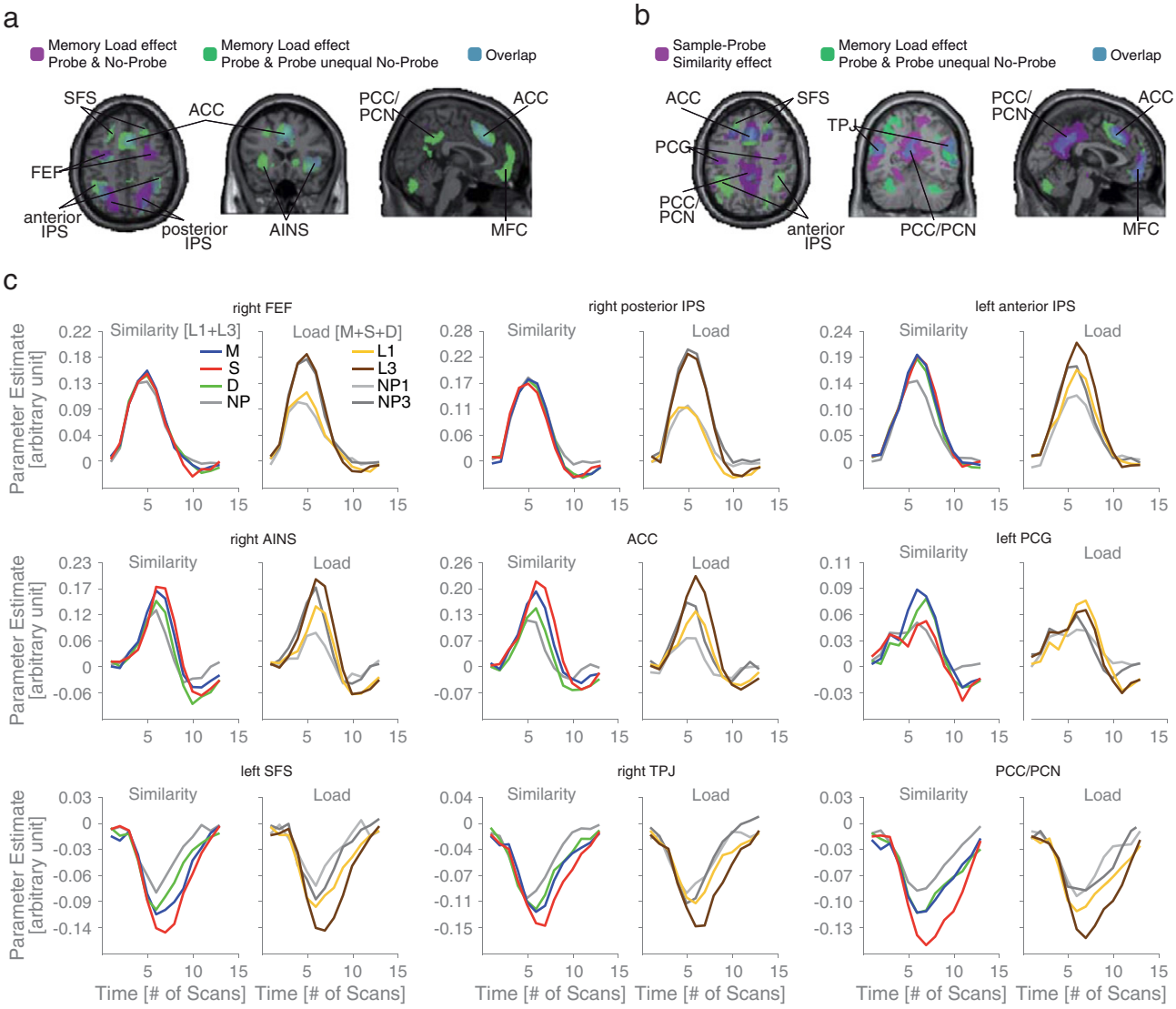

Fig. 2. Brain activation related to memory load and sample-probe-similarity. (a) Activations related to encoding/maintenance but not to recognition (purple; Load effect Probe & No-Probe) (conjunction between memory load effect in probe (with recognition) and no-probe trials (without recognition), FDR corrected at $p < 0.05$) and load-related activations contributing to recognition (green; Load effect Probe & Probe unequal No-Probe) (conjunction between memory load effect in probe trials and different activation in probe versus no-probe trials, FDR corrected at $p < 0.05$). Areas of overlap are shown in turquoise. (b) Activations specifically responsive to sample-probe manipulation during recognition (purple; Similarity) (main effect of sample-probe similarity; FDR corrected at $p < 0.05$), for comparison, again superimposed on load-related activations contributing to recognition (green, see above). Areas of overlap are shown in turquoise. (c) Activation time courses in selected brain regions associated with differentiable contributions to recognition: (first row) Right FEF and right posterior IPS were similarly modulated in probe and no-probe trials, hence, were not related to recognition and left anterior IPS that was involved in recognition but did not respond to specific recognition demands; (second row) Right AINS and ACC were modulated by memory load and sample-probe similarity with positive BOLD response ordered according to task difficulty (not specific to recognition) and left PCG suggested an effector-specific component of decision making during recognition; (third row) Left SFS, right TPJ and PCC/PCN showed negative BOLD effects that were ordered according to recognition difficulty but without a memory load effect in no-probe trials. Left panel shows BOLD responses to match (M), similar (S), dissimilar (D) probes and no-probe (NP) trials averaged across memory load 1 (L1) and memory load 3 (L3), respectively, while right panel depicts BOLD responses BOLD responses for probe trials in memory load 1 (L1) and memory load 3 (L3) averaged across the different probe types (M, S, and D), respectively, and for no-probe trials in memory load 1 (NP1) and memory load 3 (NP3), for each region respectively. Abbreviations: ACC = anterior cingulate cortex; AINS = anterior insula; FEF = frontal eye fields; IPS = intraparietal sulcus; MFC = medial frontal cortex; PCC/PCN = posterior cingulate cortex/precuneus; PCG = postcentral gyrus; SFS = superior frontal sulcus; TPJ = temporoparietal junction.

contrast, a memory load effect in probe, but not in no-probe trials, is most likely attributable to recognition, but not encoding or delay.

The first set of regions comprised bilateral anterior IPS and FEF, anterior cingulate cortex/pre-supplementary motor area (ACC, PSMA), right anterior insula (AINS) and left inferior frontal gyrus (IFG) that displayed a main effect of memory load, a stronger activation in probe compared to no-probe trials and an additional effect of memory load in no-probe trials ($p < 0.001$, uncorrected). Fig. 2c illustrates this activation pattern in left anterior IPS (first row, right panel) and in right AINS and ACC (second row, left and middle panels). Interestingly, effects in anterior portions of IPS and FEF were in obvious contrast with the abovementioned absence of activation differences in posterior IPS (Fig. 2c; first row, middle panel) that indicates functional differentiation within the IPS, with anterior portions contributing to recognition. Second, in several regions memory load effects in probe trials were not accompanied by substantial effects in no-probe trials ($p > 0.1$, uncorrected). These comprised bilateral TPJ, PCC/PCN, peri- and subgenual medial frontal cortex (MFC), superior frontal sulcus (SFS), inferior and middle temporal gyri (ITG, MTG), all exhibiting stronger negative BOLD responses under high memory load. Subcortical activations were evident in the thalamus. Fig. 2c (third row) depicts this activation pattern in three exemplary regions (left SFS, right TPJ, PCC/PCN).

However, perhaps the most convincing evidence for a role in recognition may be obtained from testing the interaction between memory load and the need for recognition. This interaction analysis revealed that TPJ, PCC/PCN, MFC, SFS and MTG showed a substantial memory

Table 1
List of cortical activations related to memory load.

Brain region	Side	MNI coordinates	Z-score
	L/R	(x, y, z in mm)	
Conjunction of load effect in probe and no-probe trials			
AINS	L	−44, 14, 1	3.95
	L	−34, 14, −2	3.46
	R	42, 20, −2	5.2
	R	36, 16, −11	4.78
	R	32, 22, 3	3.96
ACC	R	6, 20, 40	6.28
	R	9, 33, 25	5.17
	R	2, 11, 48	4.87
MFG	R	38, 44, 18	5.03
	R	36, 50, 6	4.74
	R	38, 36, 22	4.49
FEF	L	−33, −1, 51	6.28
	L	−24, −1, 42	4.58
	L	−34, −3, 37	4.58
	R	32, −3, 45	6.58
	R	28, 0, 52	6.14
	R	27, 2, 39	4.89
IPS/SPL	L	−22, −63, 58	>8
	L	−21, −69, 37	>8
	L	−32, −60, 54	>8
	R	18, −64, 56	>8
	R	26, −57, 48	7.72
	R	24, −57, 60	7.28
PCN	L	−8, −63, 21	3.46
	L	−15, −60, 19	3.39
	R	3, −60, 16	3.64
ITG	L	−42, −64, −9	3.9
	L	−36, −58, −8	3.16
	L	−51, −66, −8	2.86
Conjunction of load effect in probe trials and probe ≠ no-probe trials			
AINS	R	33, 21, −5	>8
AINS/IFG	L	−48, 27, −3	3.57
	L	−45, 27, −14	3.55
	L	−36, 32, −15	2.88
	L	−28, 20, −0	6.85
	L	−48, 3, 34	6.82
	L	−46, 3, 24	6.19
	L	−48, 27, −3	3.57
	L	−45, 27,−14	3.55
	L	−36, 32, −15	2.88
IFG	R	57, 8, 21	3.6
	R	57, 14, 15	3.23
	R	58, 6, 10	3.17
ACC	L	−4, 9, 45	7.65
	R	3, 24, 39	>8
	R	2, 15, 46	7.8
Medial frontal	L	−8, 45, −14	5.71
	R	0, 54, −9	6.81
	R	6, 51, −14	6.4
Middle cingulate gyrus	L	−2, −16, 40	4.19
	L	−6, −24, 39	3.09
	L	−3, −30, 46	3.01
MFG	R	40, 32, 21	4.43
IFG	R	57, 32, 4	4.3
FEF	L	−32, −4, 52	>8
	L	−15, −1, 48	2.69
FEF/precentral gyrus	R	34, −4, 54	5.84
	R	26, −3, 63	2.79
	R	39, −9, 48	2.59
SFS/MFG	L	−22, 27, 39	5.93
	L	−21, 35, 34	4.16
	L	−30, 18, 42	3.15
	R	26, 30, 39	5.87
	R	26, 30, 30	3.75
	R	20, 26, 46	2.83
PCC/PCN	L	−3, −40, 37	5.72
	R	12, −46, 34	5.11
	R	6, −51, 37	4.73
TPJ	L	−38, −40, 39	>8
	L	−38, −51, 54	7.09
	L	−36, −52, 42	7.04
	L	−58, −30, 18	3.48
	R	36, −51, 37	6.06
	R	44, −33, 37	4.14
	R	46, −37, 43	3.91
TPJ/MTG	L	−44, −73, 31	6.09
	L	−52, −64, 22	5.35
	L	−45, −55, 22	5.05
	L	−54, −37, 19	2.86
	R	52, −55, 21	5.88
	R	56, −61, 25	5.71
	R	56, −57, 12	5.66
MTG	L	−56, −9, −17	4.57
	L	−60, −13, −26	4.09
	L	−52, 0, −26	3.78
	R	58, −15, −26	4.83
	R	57, −15, −15	4.31
	R	57, −7, −21	4.03
ITG	L	−51, −61, −9	4.13
	L	−48, −70, −8	2.98
Insula	R	39, 3, 7	3.37
	R	48, 0, 7	3.02
Middle occipital gyrus	L	−32, −82, 16	3.88
	L	−34, −82, 25	3.01
	L	−40, −82, 12	2.93
Superior occipital gyrus	L	−20, −96, 21	4.5
	L	−24, −90, 10	3.3
	L	−9, −90, 33	3.18
	R	27, −73, 34	5.09
	R	24, −69, 42	4.58
	R	30, −75, 24	4.46
	R	20, −91, 25	4.59
	R	10, −87, 25	3.07
	R	28, −90, 19	2.9
Cuneus	R	32, −60, 4	4.29
	R	24, −72, 6	3.47
	R	28, −51, −0	2.8
Interaction of load effect and probe vs. no-probe			
IFG	L	−54, 26, −2	4.59
	L	−54, 21, 6	3.63
	R	52, 30, −5	4.27
	R	45, 34, −3	3.55
	R	52, 38, −2	3.31
MFG/SFS	R	39, 24, 37	4.3
	R	36, 30, 33	3.86
	R	39, 15, 45	3.63
Superior medial frontal	L	−10, 50, 18	4.85
	L	−3, 48, 24	3.91
	R	9, 47, 31	4.41
	R	21, 52, 18	4.48
	R	10, 60, 12	4.2
TPJ	L	−54, −46, 34	4.78

load effect in probe, but not in no-probe trials, hence clearly indicating that these regions were specifically involved in recognition. Fig. 2c (third row) illustrates the interaction patterns in left SFS, right TPJ, PCC/PCN. The full set of coordinates is listed in Table 1 and Supplementary Table 2, third section, respectively.

In summary, activation in parts of posterior IPS and FEF, commonly activated during memory maintenance, was similar for probe and no-probe trials, and therefore does not suggest a prominent role of these regions in recognition. However, some parts of IPS and FEF, as well as AINS, ACC/PSMA and IFG revealed stronger activation in probe trials, implicating them in recognition, but showed a comparable memory load effect independent of whether recognition was demanded. In contrast, TPJ, PCC/PCN, MFC and SFS displayed more negative going BOLD responses under high memory load, which were primarily evident when recognition was required.

Effects of sample-probe-similarity

Recognition-related activations elicited by variations of sample-probe-similarity could be detected in a more straightforward manner:

as match, similar non-match and dissimilar non-match trials were identical until the onset of probe presentation, and all required recognition, all activations evident from the main effect of sample-probe-similarity can be considered as recognition-related Fig. 2b shows in purple regions exhibiting sample-probe-similarity. The full set of cortical and subcortical coordinates is listed in Table 2 and Supplementary Table 2 (fourth section), respectively. On the basis of the ordering of activation strengths elicited by the probe type (match, similar non-match and dissimilar non-match), we again separated functionally distinct activity patterns. The first functional set of regions showed a graded ordering of activations according to the observed difficulty of probe evaluation as indicated by behavioral accuracy. Specifically, in bilateral TPJ, PCC/PCN, MFC, SFS, AINS, ACC/PSMA, ITG/MTG and left DLPFC similar non-matches yielded the strongest (de-)activations, followed by matching probes, and dissimilar non-matches. Fig. 2c illustrates this activity pattern in right AINS, and ACC (second row, left and middle panel, respectively) and in left SFS, right TPJ, PCC/PCN (third row). Separate post-hoc F-tests including only a) matches and similar non-matches and b) matches and dissimilar non-matches revealed that all peak F-values in these areas were significant for the comparison of matches and similar non-matches. For the comparison of matches and dissimilar non-matches, significance at $p < 0.05$, FDR-corrected, was attained only in AINS and ACC/PSMA, whereas effects in the other regions did only exceed an uncorrected level of $p < 0.001$. These regions considerably overlapped with the identified recognition-related activations in response to increasing memory load (higher (de-) activation with higher memory load), as illustrated in Fig. 2b (regions of overlap are shown in turquoise).

In addition to these overlapping areas, activation of bilateral para-/hippocampal cortex was significantly modulated by difficulty associated with sample-probe-similarity but not by increasing memory load. Post-hoc tests again revealed significant differences between matching and similar, but non-matching probes ($p < 0.05$, FDR-corrected), but only a weaker differentiation between matches and dissimilar non-matches ($p < 0.001$, uncorrected).

A second set of regions showed stronger activations in match and dissimilar non-match trials compared to similar non-matches, thus showing a pattern clearly distinct from the aforementioned difficulty-related ordering. It included bilateral postcentral gyrus (PCG), posterior MTG, anterior SPL and putamen (all post-hoc F-tests significant at $p < 0.05$, FDR-corrected). Fig. 2c exemplifies this activity pattern in left PCG (second row, right panel).

Interaction effects of memory load and sample-probe similarity

The analysis of the interaction between memory load and sample-probe similarity did not result in any significant effects.

Summary of fMRI results

Our results suggest four differentiable contributors to recognition. (1) Parts of IPS and FEF were involved in recognition as evident from higher activation when recognition was required than when not, but did not relate to recognition demands in terms of sample-probe-similarity. (2) AINS, ACC, parts of DLPFC and IFG each were modulated by memory load and sample-probe similarity and showed a positive BOLD response that was ordered according to task difficulty. (3) A similar difficulty-related response pattern was found for PCC, TPJ, MFC, SFC, but with negative BOLD effects, and without an accompanying memory load effect in no-probe trials. These activations thus seemed confined to recognition. (4) PCG, posterior middle temporal gyrus, anterior superior parietal cortex and putamen exhibited stronger responses to matching and dissimilar non-matching trials than to similar non-match trials.

Discussion

Working memory manages the encoding, maintenance and use of mental representations. Previous neuroimaging research has primarily focused on the encoding and maintenance functions, elaborating the pivotal role of attention-related regions in frontal and parietal cortex. While previous evidence has indicated that visual recognition is subserved by different brain regions than encoding and maintenance (Zarahn et al., 2006) this is the first study dedicated to a detailed characterization of the neural correlates of recognition of visual working memory contents. In line with the theoretical view that active maintenance is accomplished by attentional mechanisms whereas recognition heavily draws on mnemonic mechanisms (McElree, 2006; Oberauer, 2002), clearly distinct activation profiles were found across regions, indicating different roles for recognition.

Neuroimaging studies have consistently reported increased activation of a "fronto-parietal working memory network" (Linden, 2007) including DLPFC, ACC, FEF and IPS with increasing memory load. Several investigations on the capacity limit of working memory attribute a dominant role to the dorsal attention network (Corbetta and Shulman, 2002), especially the IPS, where activation reflects individual memory capacity (Mitchell and Cusack, 2008; Todd and Marois, 2004; Xu and Chun, 2006). These results support the assumption that the number of items that can be held active in working memory is constrained by attentional processes (Awh et al., 2006; Gazzaley and Nobre, 2012; Ikkai and Curtis, 2011; Linden, 2007; Postle, 2006; Todd and Marois, 2004).

The present memory load-related fronto-parietal pattern of activations fully complied with previous observations. Interestingly these activations seemed largely independent of whether recognition was required or not. Specifically, large parts of posterior IPS and FEF activations did not noticeably differ between probe trials (with recognition) and no-probe trials (without recognition). Only in anterior IPS and a portion of FEF higher overall activation was observed in probe trials. As probe and no-probe trials were identical until the end of the maintenance phase and solely differed with respect to recognition demands, these results can be attributed to the recognition phase, and indicate that at least parts of IPS and FEF contribute to recognition.

Relating peak coordinates observed in the present study to previous examinations, the posterior IPS focus (converted to Talairach coordinates, $x = -22/+18$, $y = -58/-60$, $z = 57/54$) was located close to results from some prominent studies on capacity constraints in visual working memory (Todd and Marois, 2004; $x = -22/+23$, $y = -65/-59$, $z = +42/+45$; Xu and Chun, 2006; $x = -21/+23$, $y = -66/-52$, $z = +42/+45$), whereas other studies (Linden et al., 2003; $x = -36/33$, $y = -47/-46$, $z = 41/42$; Mitchell and Cusack, 2008; $x = -40$, $y = -37$, $z = 46$) have reported coordinates that were close to the location of the present anterior IPS activation (converted to Talairach coordinates, $x = -39/36$, $y = -40/-48$, $z = 39/37$). The close correspondence between coordinates clearly supports the assumption that our results refer to the same regions that map individual memory capacity. The observation that anterior IPS is the only of these regions contributing to recognition implies a novel functional fractionation.

Notably, neither posterior nor anterior IPS and FEF differentiated between matching, similar (but non-matching) and dissimilar non-matching probes. These findings accord with the conception that IPS/FEF primarily reflect attentional contributions to working memory (Awh et al., 2006; Bledowski et al., 2009; Gazzaley and Nobre, 2012; Ikkai and Curtis, 2011; Linden, 2007; Mayer et al., 2007; Mitchell and Cusack, 2008; Postle, 2006), but do not themselves code the information that is held active (Emrich et al., 2013; Lewis-Peacock et al., 2012). In consequence, we suggest that IPS/FEF activation may reflect the continuation of maintenance-related attention, helping to preserve representations for recognition. Thus, IPS/FEF may still contribute considerably to successful recognition, but most likely do not subserve the matching of sensory and memory representations that is central to recognition.

The matching mechanism has been conceptualized as a process of evidence accumulation that gives rise to the computation of the required categorical decision whether the probe stimulus matches one of the samples or not (Ratcliff, 1978). Interestingly, the same class of

Table 2
List of cortical activations related to sample-probe similarity.

Brain Region	Side	MNI coordinates	Z-score
	L/R	(x, y, z in mm)	
AINS/IFG	L	−30, 21, −6	>8
	L	−39, 17, 4	5.92
	L	−38, 27, 18	4.81
	R	32, 26, −5	>8
	R	42, 32, 15	7.01
	R	42, 24, 12	4.84
ACC/medial frontal	L	−8, 23, 39	7.53
	R	6, 24, 40	>8
	R	8, 54, −8	7.21
IFG	L	−38, 39, 3	4.3
	L	−39, 32, −20	4.06
SFS/MFG	R	20, 17, 45	5.32
	R	16, 44, 33	5.14
	R	28, 29, 37	4.9
PCC/PCN	L	−4, −40, 37	6.72
	L	4, −49, 31	6.46
TPJ	L	−56, −45, 31	5.36
	R	50, −63, 27	6.4
PCG	L	−42, −13, 40	5.78
	R	36, −12, 33	5.3
ITG/MTG	L	−60, −16, −27	6.34
	L	−51, −63, 12	6.11
	L	−26, −19, −21	5.96
Cuneus	L	−16, −91, 24	4.73
	L	−22, −84, 25	3.32
	L	−30, −88, 24	3.2
Lingual gyrus	R	21, −73, −8	3.64
	R	20, −66, −11	3.57
	R	12, −67, −5	3.41

models is referred to by most investigations of perceptual decision making (e.g. Philiastides et al., 2006; Ratcliff et al., 2009), where decisions are not made on the basis of sample-probe comparisons, but mostly reflect the degree of concordance between a presented stimulus and a mental template of the target stimulus category, such as faces versus houses. Quite similar to evidence accumulation and utilization of this information for computing the decision, another family of models, summed similarity models (Nosofsky, 1988), conceive matching as a process of summing the similarity of all samples to the probe and forming a decision by comparing summed similarity to a criterion level of evidence required to answer "yes, the probe corresponds to one of the samples". In a previous magnetoencephalographic (MEG) study we used the same paradigm as presented here, but without no-probe trials (Bledowski et al., 2012). Exploiting the high temporal resolution of MEG signals we found that early event-related responses over frontal sensors gave a graded representation of sample-probe similarity (match > similar non-match > dissimilar non-match), whereas later time points reflected the categorical decision (match > similar non-match = dissimilar non-match). For fMRI, one could likewise expect a similarity-based grading of responses. Indeed, higher responses to matches compared to non-matches were found in a previous study by Rahm et al. (2006) in anterior insular and lateral frontal cortices. However, the process of matching is thought to proceed more slowly for similar non-matches than for matching probes and for high compared to low memory loads. As the BOLD response in fMRI integrates information over time, and may additionally reflect both preparatory and online (re-)allocation of processing resources, one might alternatively expect that the most time- and resource-consuming trials should yield the highest BOLD responses. In our case this would be similar non-matches.

In accordance with this alternative, ACC/pSMA, AINS and IFG, TPJ, PCC/PCN and SFC were strongly responsive to recognition demands as captured by variation of sample-probe-similarity with a difficulty-related ordering of BOLD responses (similar non-matches > matches > dissimilar non-matches). These regions widely overlapped with those reported by Heekeren et al. (2004, 2006), supporting the conceptual similarity between working memory recognition and perceptual decision making.

ACC/pSMA, AINS and IFG displayed positive BOLD responses and, like anterior IPS and anterior FEF, additionally showed memory load effects both in probe and no-probe trials as well as higher activation in probe compared to no-probe trials. Several fMRI studies on perceptual decision making have shown a difficulty-related response profile in these regions (Grinband et al., 2006; Philiastides et al., 2006). In their review Heekeren et al. (2008) pointed out that activation of ACC/pSMA, AINS and IFG signals uncertainty and the need for additional resources when an ambiguous probe is matched to a target category. Yet, other studies have suggested a more direct relation to the matching process. For example AINS has been proposed to accumulate evidence in perceptual decision making (Ho et al., 2009), or to form part of a set of regions signaling the moment of recognition (Ploran et al., 2007). Also a previous working memory study (Rahm et al., 2006) has interpreted AINS activation in terms of target detection. Given the responsiveness of ACC/pSMA and AINS to most paradigms and the limitations of the fMRI methodology (Poldrack, 2011), its exact function will most likely remain an issue of controversy. We do note however that ACC/pSMA and AINS were active during both maintenance (as indicated by the memory load effect in no-probe trials) and recognition (as indicated by the higher activation in probe compared to no-probe trials). Their response profile thus suggests that activations were not specific for recognition.

The most promising candidates to specifically represent the process of matching were found in the second set of regions that included TPJ, PCC/PCN, ITG/MTG and SFS. Here effects were observed for both manipulations of recognition difficulty: when memory load increased, activation in probe trials changed only when recognition was required. This was statistically indicated by the presence of a significant interaction between memory load and the need for recognition (probe vs. no-probe trials) in the absence of significant memory load effects in no-probe trials even at a liberal, uncorrected threshold of $p < 0.1$. With respect to sample-probe similarity, most deactivation was observed in trials where similar but non-matching probes were presented, followed by matching probes and dissimilar non-matches. In accordance with these results, a previous study from our group has reported deactivation of TPJ, PCC/PCN and SFS in the context of selecting a memory item in working memory on the basis of an indirect cue, which was hypothesized to include the retrieval of the representation (Bledowski, Rahm and Rowe, 2009). Again, a quite similar set of regions has been reported in several previous studies on perceptual decision making (Heekeren et al., 2004, 2006), and also on recognition from long-term memory (Wagner et al., 2005).

However, the active role in decision making attributed to these regions was put into question with referral to their ubiquitous activation in the "default mode" (Raichle et al., 2001) raising serious doubts about whether their deactivation may be epiphenomenal to global cognitive demands (Ho et al., 2009; Tosoni et al., 2008). However, recent data from Philiastides et al. (2011) strongly disagree with this objection: in their study the perturbation of activity in the SFS with transcranial magnetic stimulation reduced the speed and accuracy of perceptual decisions, demonstrating a crucial role of SFS in decision making. Moreover, the current results cannot be exhaustively explained by global cognitive demands due to increased task difficulty. Rather, at least part of the deactivation appeared rather specifically modulated by recognition. That is, parts of TPJ and PCC/PCN did not exhibit any memory load effect in no-probe trials that would have been due to earlier task phases. Thus, these deactivations were not driven by global task demands, but selectively by demands on recognition. In line with these results, Mayer et al. (2010) demonstrated a fractionation of the default mode network by variation of attentional as opposed to working memory demands. Areas that were selectively involved in working memory processing at least in the right hemisphere included SFS, medial frontal areas and TPJ, supporting the assumption that default mode regions in

the context of working memory are not functionally uniform, which is in strong contrast to the suggestion that their deactivation reflects global task difficulty.

But why are responses negative, and what may this tell us about their function? Recent studies have indicated that the physiological basis of negative BOLD is indeed decreased neural activity, as evident from macaque intracranial recordings (Hayden et al., 2009), depth electrode recordings in humans (Ossandón et al., 2011), and accordingly reduced local cerebral metabolic rate of oxygen (Lin et al., 2011). Reductions in neuronal activity were proposed to result from inhibitory local or long-range interactions. For default mode regions, it has been suggested that their deactivation originates from inhibitory projections from task-relevant activated regions (Anticevic et al., 2012; Mayer et al., 2010), which would also explain why default mode regions were selectively modulated to task demands, as observed here.

Functionally, default mode regions are commonly thought to support self-referential processing (Buckner et al., 2008). Suppressing internally directed activity may help to optimize cognitive functions directed to external stimuli. Thus, the efficiency of goal-directed behavior may depend on the interplay between activation and deactivation between regions. This still leaves room for specific functions of regions showing activation decreases. For example, Shulman et al. (2007) hypothesized that deactivation of TPJ indicates the degree of filtering irrelevant information. Such a filtering mechanism may as well contribute to perceptual and working memory matching. More negative going neural responses would then be expected for non-matching compared to matching information. In our study accuracy and response times differed between matches and non-matches, which most likely entailed longer durations of matching/filtering. We therefore cannot assess this hypothesis directly. However, studies on the old/new effect in long-term memory have consistently reported higher activation for studied (that is matching) items compared to unstudied (non-matching) ones (see meta-analysis by Kim, 2013), pointing to the same direction.

In contrast to negative BOLD regions potentially implicated in matching, we observed another set of regions comprising PCG and anterior regions of lateral parietal cortex that were affected by the sample-probe manipulation. These were readily differentiable from the previously mentioned activations by their profile across probe types and the absence of any noticeable memory load effect. Specifically, both matches and dissimilar non-matches yielded comparable activations that were more strongly positive than for similar non-matches. Activations in PCG, probably motor cortex, appeared bilaterally even though the motor response was always made with the right hand and were also evident in no-probe trials that did not require manual responding at all, and in consequence are unlikely to directly relate to motor execution. Rather they may reflect an effector-specific component of decision making, as suggested by both electrophysiological studies in monkeys (Gold and Shadlen, 2000; Hernandez et al., 2002; Romo et al., 2002) and human neuroimaging (Tosoni et al., 2008). In particular, these studies have provided evidence for the existence of sensory–motor mechanisms that integrate evidence in favor of the effector-specific decision outcome. I.e., Tosoni et al. (2008) had their participants decide whether a noisy stimulus pictured a face or a house, indicating their decision by eye- vs. hand-pointing movements. Results convincingly demonstrated that activation in saccade- vs. pointing selective regions gradually reflected the amount of evidence in favor of their currently associated stimulus category (face vs. house). Relating these results to the present study, here, both alternatives (match vs. non-match) mapped on the same effector, a movement of the right hand. Most evidence in favor of match vs. non-match responses could be extracted from matching and clearly dissimilar probes – which yielded the strongest activation – whereas similar but non-matching probes were most ambiguous and associated with a weaker brain response. The present results hence comply with Tosoni et al.'s proposal. However, if activations represented evidence per se, one might have expected lower responses in the more difficult high-memory load condition. While no significant effect of memory load was evident, at least in left PCG memory load 1 descriptively showed higher peak activation than memory load 3, which may be seen as an additional weak hint in favor of the interpretation of our results in the light of perceptual decision making. However, whether the computations reflected in these activations relate to the absolute amount of evidence, or rather to the current relation of evidence in favor of one versus the other response alternative, cannot unequivocally be decided neither on the basis of Tosoni's nor our data.

Despite close correspondence in many regions, the present study also revealed differences to studies of perceptual decision making. Especially, previous studies by Heekeren et al. (2004, 2006) have reported increased activation in the dorsal attention network, especially FEF and IPS, with increasing stimulus ambiguity. In contrast, our results showed that their activation increased with memory load, but did not relate to sample-probe similarity. This difference most likely originated from the different experimental approaches: perceptual decision making is typically studied by use of visually degraded pictures. Increasing attentional effort to support their detailed inspection may help to disambiguate their content. In contrast, the working memory probes in the present study consisted of uniformly colored squares. Their information content is readily available, and – as all colors were easily discriminable when presented simultaneously – the process of matching and its difficulty seems likely to be determined by the quality of the samples' mnemonic representations rather than by the probe stimulus.

Conclusion

Working memory is conceived as emerging from the interaction of attentional and mnemonic resources. However, as neuroimaging studies have primarily focused on the encoding and maintenance functions of visual working memory, it has remained unclear whether this conception provides a sufficient basis for recognition. Here, we sought to provide a detailed characterization of working memory recognition. As expected, recognition strongly draws on brain regions implicated in mnemonic processing, and less on attentional processing. To a large extent, our working memory results paralleled evidence from studies on perceptual decision making, which likely reflects the conceptual similarity in the mechanism of matching information in both domains. We suggest that the conception of working memory as relying on attentional and mnemonic subprocesses should be extended to explicitly account for mechanisms of decision making in memory.

Supplementary data to this article can be found online at http://dx.doi.org/10.1016/j.neuroimage.2013.12.017.

Acknowledgments

This study was supported by the Frankfurt Medical Faculty Intramural Young Investigator Program to Christoph Bledowski. We thank Katharina Spira for helping to test the color stimuli and Christian Altmann for advice on presentation software.

Conflict of interest

The authors declare that the research was conducted in the complete absence of conflicting financial or commercial interests.

References

Anticevic, A., Cole, M.W., Murray, J.D., Corlett, P.R., Wang, X.J., Krystal, J.H., 2012. The role of default network deactivation in cognition and disease. Trends Cogn. Sci. 16, 584–592.

Ashburner, J., 2007. A fast diffeomorphic image registration algorithm. Neuroimage 38, 95–113.

Awh, E., Vogel, E.K., Oh, S.H., 2006. Interactions between attention and working memory. Neuroscience 139, 201–208.

Baddeley, A.D., 1986. Working Memory. Clarendon Press; Oxford University Press, Oxford Oxfordshire New York.

Bledowski, C., Cohen Kadosh, K., Wibral, M., Rahm, B., Bittner, R.A., Hoechstetter, K., Scherg, M., Maurer, K., Goebel, R., Linden, D.E., 2006. Mental chronometry of working memory retrieval: a combined functional magnetic resonance imaging and event-related potentials approach. J. Neurosci. 26, 821–829.
Bledowski, C., Rahm, B., Rowe, J.B., 2009. What "works" in working memory? Separate systems for selection and updating of critical information. J. Neurosci. 29, 13735–13741.
Bledowski, C., Kaiser, J., Wibral, M., Yildiz-Erzberger, K., Rahm, B., 2012. Separable neural bases for subprocesses of recognition in working memory. Cereb. Cortex 22, 1950–1958.
Buckner, R.L., Andrews-Hanna, J.R., Schacter, D.L., 2008. The brain's default network: anatomy, function, and relevance to disease. Ann. N. Y. Acad. Sci. 1124, 1–38.
Corbetta, M., Shulman, G.L., 2002. Control of goal-directed and stimulus-driven attention in the brain. Nat. Rev. Neurosci. 3, 201–215.
Cowan, N., 2005. Working Memory Capacity. Psychology Press, New York.
Emrich, S.M., Riggall, A.C., Larocque, J.J., Postle, B.R., 2013. Distributed patterns of activity in sensory cortex reflect the precision of multiple items maintained in visual short-term memory. J. Neurosci. 33, 6516–6523.
Gazzaley, A., Nobre, A.C., 2012. Top-down modulation: bridging selective attention and working memory. Trends Cogn. Sci. 16, 129–135.
Gold, J.I., Shadlen, M.N., 2000. Representation of a perceptual decision in developing oculomotor commands. Nature 404, 390–394.
Grinband, J., Hirsch, J., Ferrera, V.P., 2006. A neural representation of categorization uncertainty in the human brain. Neuron 49, 757–763.
Hayden, B.Y., Smith, D.V., Platt, M.L., 2009. Electrophysiological correlates of default-mode processing in macaque posterior cingulate cortex. Proc. Natl. Acad. Sci. U. S. A. 106, 5948–5953.
Heekeren, H.R., Marrett, S., Bandettini, P.A., Ungerleider, L.G., 2004. A general mechanism for perceptual decision-making in the human brain. Nature 431, 859–862.
Heekeren, H.R., Marrett, S., Ruff, D.A., Bandettini, P.A., Ungerleider, L.G., 2006. Involvement of human left dorsolateral prefrontal cortex in perceptual decision making is independent of response modality. Proc. Natl. Acad. Sci. U. S. A. 103, 10023–10028.
Heekeren, H.R., Marrett, S., Ungerleider, L.G., 2008. The neural systems that mediate human perceptual decision making. Nat. Rev. Neurosci. 9, 467–479.
Hernandez, A., Zainos, A., Romo, R., 2002. Temporal evolution of a decision-making process in medial premotor cortex. Neuron 33, 959–972.
Ho, T.C., Brown, S., Serences, J.T., 2009. Domain general mechanisms of perceptual decision making in human cortex. J. Neurosci. 29, 8675–8687.
Ikkai, A., Curtis, C.E., 2011. Common neural mechanisms supporting spatial working memory, attention and motor intention. Neuropsychologia 49, 1428–1434.
Kahana, M.J., Sekuler, R., 2002. Recognizing spatial patterns: a noisy exemplar approach. Vis. Res. 42, 2177–2192.
Kaiser, J., Lutzenberger, W., Decker, C., Wibral, M., Rahm, B., 2009a. Task- and performance-related modulation of domain-specific auditory short-term memory representations in the gamma-band. Neuroimage 46, 1127–1136.
Kaiser, J., Rahm, B., Lutzenberger, W., 2009b. Temporal dynamics of stimulus-specific gamma-band activity components during auditory short-term memory. Neuroimage 44, 257–264.
Kim, H., 2013. Differential neural activity in the recognition of old versus new events: an activation likelihood estimation meta-analysis. Hum. Brain Mapp. 34, 814–836.
Lepsien, J., Nobre, A.C., 2007. Attentional modulation of object representations in working memory. Cereb. Cortex 17, 2072–2083.
Lewis-Peacock, J.A., Drysdale, A.T., Oberauer, K., Postle, B.R., 2012. Neural evidence for a distinction between short-term memory and the focus of attention. J. Cogn. Neurosci. 24, 61–79.
Lin, P., Hasson, U., Jovicich, J., Robinson, S., 2011. A neuronal basis for task-negative responses in the human brain. Cereb. Cortex 21, 821–830.
Linden, D.E., 2007. The working memory networks of the human brain. Neuroscientist 13, 257–267.
Linden, D.E., Bittner, R.A., Muckli, L., Waltz, J.A., Kriegeskorte, N., Goebel, R., Singer, W., Munk, M.H., 2003. Cortical capacity constraints for visual working memory: dissociation of fMRI load effects in a fronto-parietal network. Neuroimage 20, 1518–1530.
Maldjian, J.A., Laurienti, P.J., Kraft, R.A., Burdette, J.H., 2003. An automated method for neuroanatomic and cytoarchitectonic atlas-based interrogation of fMRI data sets. Neuroimage 19, 1233–1239.
Mayer, J.S., Bittner, R.A., Nikolic, D., Bledowski, C., Goebel, R., Linden, D.E., 2007. Common neural substrates for visual working memory and attention. Neuroimage 36, 441–453.
Mayer, J.S., Roebroeck, A., Maurer, K., Linden, D.E., 2010. Specialization in the default mode: task-induced brain deactivations dissociate between visual working memory and attention. Hum. Brain Mapp. 31, 126–139.
McElree, B., 2006. Accessing recent events. In: Ross, B.H. (Ed.), The psychology of learning and motivation, Vol. 46. Academic Press, San Diego.
Mitchell, D.J., Cusack, R., 2008. Flexible, capacity-limited activity of posterior parietal cortex in perceptual as well as visual short-term memory tasks. Cereb. Cortex 18, 1788–1798.
Nosofsky, R.M., 1988. Exemplar-based accounts of relations between classification, recognition and typicality. J. Exp. Psychol. Learn. Mem. Cogn. 14, 9.
Oberauer, K., 2002. Access to information in working memory: exploring the focus of attention. J Exp Psychol Learn Mem Cogn. 28, 411–421.
Ossandón, T., Jerbi, K., Vidal, J.R., Bayle, D.J., Henaff, M.A., Jung, J., Minotti, L., Bertrand, O., Kahane, P., Lachaux, J.P., 2011. Transient suppression of broadband gamma power in the default-mode network is correlated with task complexity and subject performance. J. Neurosci. 31, 14521–14530.
Philiastides, M.G., Ratcliff, R., Sajda, P., 2006. Neural representation of task difficulty and decision making during perceptual categorization: a timing diagram. J. Neurosci. 26, 8965–8975.
Philiastides, M.G., Auksztulewicz, R., Heekeren, H.R., Blankenburg, F., 2011. Causal role of dorsolateral prefrontal cortex in human perceptual decision making. Curr. Biol. 21, 980–983.
Ploran, E.J., Nelson, S.M., Velanova, K., Donaldson, D.I., Petersen, S.E., Wheeler, M.E., 2007. Evidence accumulation and the moment of recognition: dissociating perceptual recognition processes using fMRI. J. Neurosci. 27, 11912–11924.
Poldrack, R.A., 2011. Inferring mental states from neuroimaging data: from reverse inference to large-scale decoding. Neuron 72, 692–697.
Postle, B.R., 2006. Working memory as an emergent property of the mind and brain. Neuroscience 139, 23–38.
Rahm, B., Opwis, K., Kaller, C.P., Spreer, J., Schwarzwald, R., Seifritz, E., Halsband, U., Unterrainer, J.M., 2006. Tracking the subprocesses of decision-based action in the human frontal lobes. Neuroimage 30, 656–667.
Raichle, M.E., MacLeod, A.M., Snyder, A.Z., Powers, W.J., Gusnard, D.A., Shulman, G.L., 2001. A default mode of brain function. Proc. Natl. Acad. Sci. U. S. A. 98, 676–682.
Ratcliff, R., 1978. A theory of memory retrieval. Psychol. Rev. 85, 49.
Ratcliff, R., Philiastides, M.G., Sajda, P., 2009. Quality of evidence for perceptual decision making is indexed by trial-to-trial variability of the EEG. Proc. Natl. Acad. Sci. U. S. A. 106, 6539–6544.
Romo, R., Hernandez, A., Zainos, A., Lemus, L., Brody, C.D., 2002. Neuronal correlates of decision-making in secondary somatosensory cortex. Nat. Neurosci. 5, 1217–1225.
Shulman, G.L., Astafiev, S.V., McAvoy, M.P., d'Avossa, G., Corbetta, M., 2007. Right TPJ deactivation during visual search: functional significance and support for a filter hypothesis. Cereb. Cortex 17, 2625–2633.
Sternberg, S., 1966. High-speed scanning in human memory. Science 153, 652–654.
Todd, J.J., Marois, R., 2004. Capacity limit of visual short-term memory in human posterior parietal cortex. Nature 428, 751–754.
Tosoni, A., Galati, G., Romani, G.L., Corbetta, M., 2008. Sensory–motor mechanisms in human parietal cortex underlie arbitrary visual decisions. Nat. Neurosci. 11, 1446–1453.
Xu, Y., Chun, M.M., 2006. Dissociable neural mechanisms supporting visual short-term memory for objects. Nature 440, 91–105.
Wagner, A.D., Shannon, B.J., Kahn, I., Buckner, R.L., 2005. Parietal lobe contributions to episodic memory retrieval. Trends Cogn. Sci. 9, 445–453.
Zaitsev, M., Hennig, J., Speck, O., 2004. Point spread function mapping with parallel imaging techniques and high acceleration factors: fast, robust, and flexible method for echo-planar imaging distortion correction. Magn. Reson. Med. 52, 1156–1166.
Zarahn, E., Rakitin, B.C., Abela, D., Flynn, J., Stern, Y., 2006. Distinct spatial patterns of brain activity associated with memory storage and search. Neuroimage 33, 794–804.